LBL-15231 Rev.
Preprint c.2

Lawrence Berkeley Laboratory
UNIVERSITY OF CALIFORNIA

Materials & Molecular Research Division

RECEIVED
LAWRENCE
BERKELEY LABORATORY

FEB 21 1984

LIBRARY AND
DOCUMENTS SECTION

Submitted to Surface Science

HIGH COVERAGE STATES OF OXYGEN ADSORBED ON Pt(100) AND Pt(111) SURFACES

G.N. Derry and P.N. Ross

December 1983

TWO-WEEK LOAN COPY

This is a Library Circulating Copy which may be borrowed for two weeks. For a personal retention copy, call Tech. Info. Division, Ext. 6782.

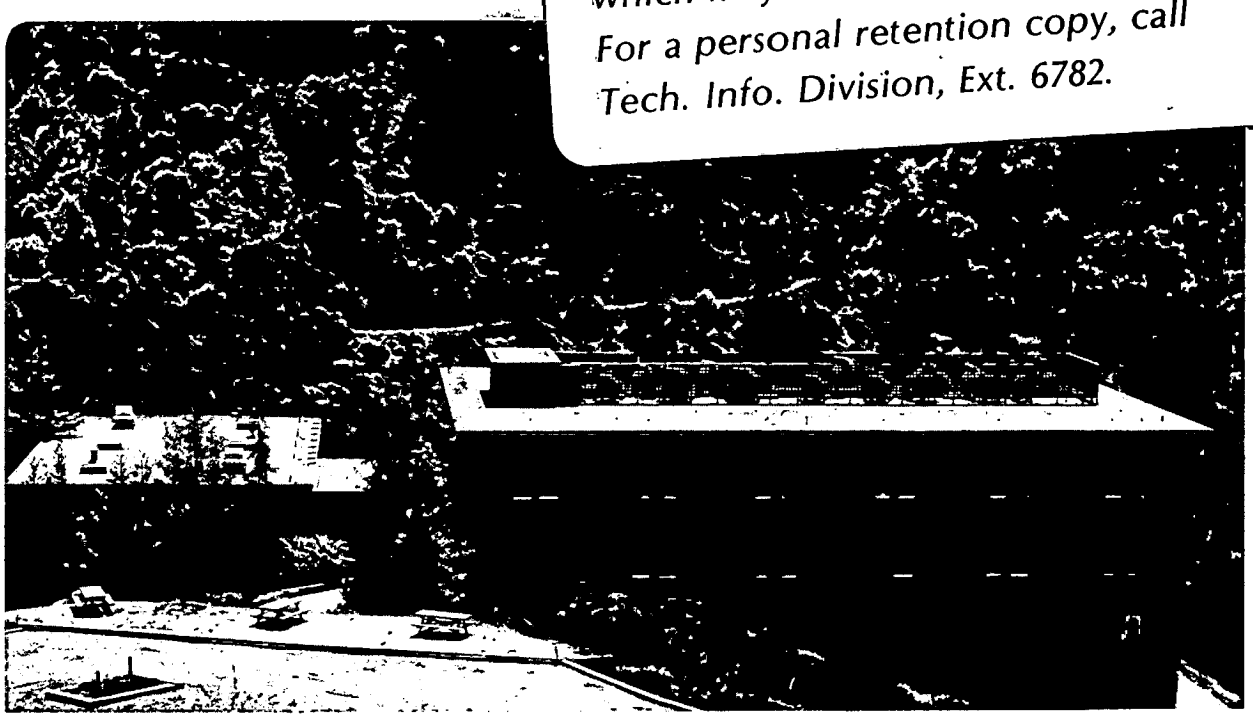

Prepared for the U.S. Department of Energy under Contract DE-AC03-76SF00098

LBL-15231 Rev. c.2

DISCLAIMER

This document was prepared as an account of work sponsored by the United States Government. While this document is believed to contain correct information, neither the United States Government nor any agency thereof, nor the Regents of the University of California, nor any of their employees, makes any warranty, express or implied, or assumes any legal responsibility for the accuracy, completeness, or usefulness of any information, apparatus, product, or process disclosed, or represents that its use would not infringe privately owned rights. Reference herein to any specific commercial product, process, or service by its trade name, trademark, manufacturer, or otherwise, does not necessarily constitute or imply its endorsement, recommendation, or favoring by the United States Government or any agency thereof, or the Regents of the University of California. The views and opinions of authors expressed herein do not necessarily state or reflect those of the United States Government or any agency thereof or the Regents of the University of California.

HIGH COVERAGE STATES OF OXYGEN

ADSORBED ON Pt(100) AND Pt(111) SURFACES

G. N. Derry[†] and P. N. Ross

Lawrence Berkeley Laboratory
Materials and Molecular Research Division
University of California
Berkeley, CA 94720

ABSTRACT

Oxygen adsorption on the Pt(100) and Pt(111) surfaces was investigated using x-ray photoemission and thermal desorption spectroscopies. Low pressure (ca. 10^{-5} Pa) oxygen dosing at near ambient crystal temperature resulted in the formation of dissociated adsorbed species at saturation coverages of nominally 0.2-0.25 monolayer on both surfaces. The combination of higher pressure (ca. 10^{-3} Pa) and higher surface temperature (570 K) dosing produced a three to five times higher saturation coverage than the low pressure dosing. The effect of dosing condition on the saturation coverage appears to reconcile apparent discrepancies for the Pt(100) surface in the literature. Characterization by XPS of the higher coverage state for oxygen showed that it is in the same chemical state as the oxygen adsorbed at very low coverage. Angle-resolved XPS has shown that in all cases the oxygen appears to reside on the surface with no significant penetration of oxygen into the bulk, as would be characteristic of oxidation. However, some penetration on the surface by oxygen, such as by a place-exchange type restructuring of the first two atomic layers, cannot be entirely ruled out.

[†]Present address: Department of Physics, University of North Carolina Chapel Hill, North Carolina 27514.

I. Introduction

The interaction of oxygen with a platinum surface has long been an important problem in surface science. The motivation for such extensive study of this system is both a pragmatic desire to understand the catalytic and electrochemical properties of this technologically important material and intrinsic fundamental interest in the physics and chemistry of the interactions of oxygen with the surfaces of the Group VIII metals. There have been numerous previous studies of oxygen adsorption on platinum surfaces, but in many instances the results have either been inconsistent or else have not been repeated. In some cases, however, the results are consistent and some aspects of the problem are beginning to be understood.

Norton and co-workers reported photoemission (XPS and UPS) studies of oxygen interactions with polycrystalline platinum (1,2), supported Pt catalysts (3), and the Pt(100) surface (3). The results of the latter study were interpreted as formation of bulk-like platinum oxides at high O_2 pressure ($\sim 10^3$ Pa) and sample temperature (550 K) at both the single crystal and supported catalyst surface. No other attempts to treat single crystal Pt at such high pressures have been reported.

The adsorption of oxygen at low pressure on the Pt(111) surface has been extensively studied, most recently by Gland, et al. (4,5), Monroe and Merrill (6), and Campbell, et al. (7). The results of these works are fairly consistent, the consensus being that oxygen adsorbs dissociatively on Pt(111) at room temperature via a molecular precursor state and forms an ordered layer with a (2x2) LEED pattern and a saturation coverage 0.25 monolayer. Some aspects of the UPS of oxygen on

Pt are more controversial, however, in particular, the interpretation of O2p emission in evaluating the nature of oxygen bonding on different transition metal surfaces (8,9,10,11). Another controversial topic has been oxygen adsorption on the Pt(100) surface. The clean surface reconstructs upon vacuum annealing to exhibit a (5x20) LEED pattern. Helms, et al. (12), and Pirug, et al. (13) have prepared a clean Pt(100)-(1x1) surface by following a specified sequence of gas exposures and surface temperatures. They found the initial sticking coefficient for oxygen to be higher on the (1x1) than on the (5x20) surface. Results of cluster calculations (SCF-Xα-SW) by Balazs and Johnson (14) are consistent with this result. The experimental situation for oxygen adsorption on Pt(100) -(5x20) is not clear, however. Kneringer and Netzer (15) studied this system using thermal desorption and LEED, as did Barteau, Ko, and Madix (16). The results of these two investigations were different in almost every respect. The thermal desorption lineshapes were radically different; Barteau, et al. reported a significantly higher saturation coverage; and the LEED results do not agree. The dosing pressure and surface temperature were, however, very different, and this may have had an important effect on the results. One of the motivations for our study was to see whether we could reconcile these very different results on Pt(100).

In this work, we characterize the oxygen adsorbate layer formed on Pt(111) and Pt(100) under widely varying conditions of oxygen pressure and surface temperature using complementory information from two surface spectroscopies, viz., XPS, and thermal desorption mass spectroscopy (TDS). The effect of surface structure is examined by using two different crystal faces, (111) and (100), but no LEED analysis was

performed. We did not employ the special procedures to prepare a clean Pt(100)-(1x1) surface, so the designation Pt(100) we use hereafter should be taken to mean the reconstructed surface. Results for different dosing conditions were used to evaluate the discrepancies concerning O_2/Pt(100) discussed above. The question of oxide formation, as described by Norton and co-workers, was examined by using angle-resolved XPS data to provide information on the penetration of oxygen below the Pt surface.

II. Experimental

The experiments were carried out in an ultra-high vacuum chamber equipped with an x-ray source, UV lamp, mass spectrometer, ion gun, hermispherical electron spectrometer, and sample manipulator. The chamber is pumped by an ion pump and a titanium sublimation pump, and has a nominal base pressure of $\approx 1 \times 10^{-8}$ Pa. The x-ray tube, UV lamp, and ion gun are all commercial devices from Physical Electornics. The x-ray tube employs a magnesium anode, producing unmonochromatized MgKα radiation ($h\nu$ = 1253.6 eV). The UV lamp is of the He cold cathode discharge type, also unmonochromatized. The electron spectrometer is a hemispherical analyzer with a microchannel plate at the detector end and a double einzel lens at the entrance. This arrangement allows good angular resolution ($\approx 3°$) while maintaining reasonable energy resolution and count rates. This angular resolution allows variable surface sensitivity (17) by changing the angle between the surface and the lens axis (see Fig. 1). The timing and coordination of the data acquisition are controlled by an LSI-11 microprocessor and related peripherals. The computer was also used to digitally smooth the data for display.

The reference level for binding energies measured in this work is the platinum Fermi level, located empirically by using the inflection point in the onset of valence band emission. Experimentally, there is uncertainty in the location of E_F itself and possible small non-linearities in the programmable ramp voltage (18). We estimate the uncertainty in the absolute binding energy to be about 0.6 eV. Relative binding energy changes are more accurate, the major uncertainty being location of the peak in wide, noisy, or asymmetric spectra. We estimate the uncertainty in the energy shifts to be about 0.2 eV in the worst case.

The quadruple mass spectrometer is an Inficon IQ 200 with 10 mass-channel analog outputs. The thermal desorption experiment is also under computer control. The LSI-11 runs a programmable power supply, while the mass-channel outputs and amplified thermocouple signal are digitized and stored in memory. A simple feedback loop promotes linearity of the temperature ramp. Data presented in this study were taken using a heating rate of ≈10 K/sec. The crystals are mounted onto a small 40 W heater by means of a tantalum cup (Varian sample holder Model 981-2526), and the temperature is measured by a Pt-Pt/Rh thermocouple spotwelded to the side of the crystal. The crystals are slices cut from 0.635 cm diameter [001] and [111] oriented rods and mechanically polished by standard techniques. Prior to mounting in the vacuum system, they were annealed at 1200 K in air for 16 hrs and chemically etched with aqua regia. Surface preparation *in vacuo* followed the usual methods: cycles of argon ion bombardment, heating in oxygen, and high temperature annealing. No contaminants were seen with XPS after this treatment.

The oxygen (99.997%) is introduced through a dosing tube attached to a precision leak valve. This tube has a fork to direct gas equivalently towards the sample and the mass spectrometer, permitting the effective pressure of oxygen impinging on the sample surface to be determined during "low pressure" dosing conditions. Under these conditions, high pumping speed was maintained in the vacuum system, and the difference in effective gas pressure at the face of the crystal exceeded the system pressure (as read by the ion gauge) by two orders of magnitude. For higher pressure ($\sim 10^{-3}$ Pa) dosing, however, impurity gases (especially CO) backstreaming from the ion pump necessitated partially closing off the gate valve, and

the desired total system pressure was then maintained by balancing the amounts of oxygen flowing in and being pumped out. Under these conditions the system pressure and the gas pressure at the sample are nominally the same. This method is inherently less accurate than the low pressure technique and exposure values quoted in this regime should be taken as nominal.

III. Results

A. Thermal Desorption

1. Pt(100) Surface

The first thermal desorption data we shall describe were taken for a series of exposures at a low dosing pressure ($P \approx 1.3 \times 10^{-5}$ Pa) and moderate surface temperature ($T_s \lesssim 370$ K). Oxygen dosing was started at $T_s \approx 370$ K and maintained for a time sufficient to achieve the desired exposure, during which the sample continued to cool (T_s decreased 20 K in this time interval). This procedure should be assumed whenever $T_s \lesssim 370$ K is quoted. No difference in the thermal desorption spectra was observed when equilibration to ambient temperature was used.

Mass 32 and mass 28 were monitored simultaneously to observe O_2 desorption and check for any CO contamination (which was not seen). An example of the oxygen data is shown in curve b of Fig. 3. The relative oxygen coverage is obtained by numerically integrating the digital thermal desorption data, and a plot of relative coverage increase with exposure is shown in Fig. 2a. The peak areas of the thermal desorption spectra were calibrated against a CO desorption spectrum, using the absolute calibration of Norton, et al. (19) for the saturation coverage of CO. From this calibration, we estimated the saturation coverage to be $(2.5 \pm 1.3) \times 10^{14}$ atoms/cm^2, ~ 0.2 monolayers. From the data of Fig. 2a, the initial sticking coefficient is estimated to be $S_0 \geqq 0.02$ using the lower limit of

saturation coverage. This value is higher by a factor of 10 than any quoted in the literature (15,16), a point which will be pursued further in Section IV.

The qualitative features of the thermal desorption curves are consistent with a second-order process. The line-shape is symmetrical and the peak temperature decreases with increasing coverage. The latter effect is shown in Fig. 2b, plotted in accordance with the analysis of Redhead (20). If one assumes that the desorption kinetics are governed by the Polanyi-Wigner equation.

$$-\frac{dN}{dt} = k_o N^m e^{-(E/RT)} \qquad [1]$$

where k_o and E are constants and m=2, then the slope of Fig. 2b determines E, in this case E ≈ 113 kJ/mole. A plot of ln $(\frac{dN}{dt})$ vs. $\frac{1}{T}$ at fixed coverage (variable initial coverage) also yields the desorption energy (21); this was done for six coverages and the average value is E = 119 ± 27 kJ/mole. Also a plot of ln $(\frac{dN}{dt})$ vs. ln N at fixed T has a slope equal to m, the formal reaction order. Our results are consistent with m=2, but the data have considerable scatter.

A radically different thermal desorption spectrum, curve a of Fig. 3, resulted from dosing with a relatively high oxygen pressure (P ~ 10^{-3} Pa) for 300 sec and an elevated surface temperature (T_s ≈ 570 K). The coverage increased by a factor of 3-5, and the conditions for which curves a and b are characteristic in Fig. 3 will be referred to as the "high coverage" and "low coverage" regimes, respectively. Correspondingly, the states of adsorbed oxygen on this surface which produce the desorption spectra characterized by Figs. 3a and b will be referred to as the "high

coverage" and "low coverage" states. Several desorption spectra were recorded for oxygen exposure under the same nominal conditions (the surface temperature could be held easily to within ± 5 K, but the O_2 pressure may have varied widely, as explained in Section II). These curves varied somewhat in detail, but all shared the same qualitative features. A steeply rising leading edge, a sharp peak at ≃ 660 K, a second peak at ≃ 703 K, and a slowly decreasing high temperature tail are all characteristic of the high coverage state.

If the sample was exposed to oxygen at low pressure ($\sim 10^{-5}$ Pa) but elevated surface temperature (≈ 570 K), the thermal desorption spectrum showed only a moderate increase in coverage, but with an asymmetric lineshape (the low temperature side rising more steeply, though not so dramatically as in the high coverage regime). Conversely, if the ambient temperature surface was exposed to high ($\sim 10^{-3}$ Pa) oxygen pressure, there was a similar asymmetry, moderate coverage increase, and about a $\lesssim$70 K lower peak temperature. Thus, while either high pressure or temperature tend to increase the coverage, it seems that both are required for the formation of the high coverage state.

2. Pt(111) Surface

Thermal desorption results for the O_2/Pt(111) system are shown in Fig. 4. Curve b is for exposure at $T_s \lesssim 370$ K, using $P \approx 1.3 \times 10^{-5}$ Pa oxygen for 300 sec. The lineshape is nearly symmetric and the coverage is similar to the O_2/Pt(100) case. The peak temperature is somewhat higher than previously reported values (4,5,7,8), which show a considerable scatter. The present value is reasonably close to the highest of these (5). The slight asymmetry was also present in some previous work (5,7). An

extensive analysis has been done for O_2/Pt(111) (4), and no attempt was made here to repeat that work. Our main interest was to ascertain the effect of surface crystal structure (if any) on the formation of the high coverage state.

This result is shown in curve a of Fig. 4, a desorption spectrum taken after dosing at $T_s \approx 570$ K for 300 sec at higher oxygen pressure ($P \approx 10^{-3}$ Pa). Clearly, these exposure conditions induce a coverage increase comparable to that shown in Fig. 3. The lineshape, however, exhibits both similarities and differences for oxygen desorption from the high coverage state of Pt(111) and Pt(100). Curve a in Fig. 4 shows an asymmetry toward lower desorption temperature and a steep rise in the leading edge. It does not have a sharp, narrow peak, however, or any multiple peak structure. Exposure conditions employing high surface temperature or high oxygen pressure, but not both, gave rise to desorption spectra very similar to those already described for O_2/Pt(100) under these conditions.

B. X-ray Photoelectron Spectroscopy

1. Pt(100) Surface

Data for the O1s line for oxygen adsorbed on Pt(100) is presented in Fig. 5. The geometry is identical for curves a and b, the take-off angle for the spectrometer being about 84° from the surface normal. Curve a was recorded after dosing for 300 sec at $P \sim 10^{-3}$ Pa O_2 and $T_s \approx 570$ K, conditions which produced the high coverage state. Spectrum b, on the other hand, was exposed to $\sim 10^{-4}$ Pa O_2 at $T_s \lesssim 370$ K for 300 sec, conditions which produced the low coverage state. The O1s photoemission intensity from the high coverage state was greater than for the low coverage state,

but the O1s peak area ratio for the two states is not the same as for the TDS peak area ratio in Fig. 3, i.e. the TDS peak area ratio is greater than the XPS peak area ratio. This difference between the TDS and XPS determinations arises from a combination of factors. The designations "high coverage" and "low coverage" are only nominal and refer to ratios in coverage that can vary from 3 to 5. It was even observed that TDS and XPS peak area ratios for identical dosing conditions were not exactly the same, the TDS ratios being the greater. This was probably due to the experimental factors, such as oxygen clean-off during the XPS collection time interval (20-30 min), or temporary changes in the vacuum system pumping speed caused by high pressure O_2 dosing. Nonetheless, as we shall show subsequently, the oxygen coverage calculated from the O1s/Pt4p ratio in Fig. 6 is in reasonable agreement with the coverage measured from the thermal desorption spectrum.

Examination of Fig. 5 reveals that curve a is shifted by ca. -0.4 eV with respect to curve b. Although this shift is small and only just resolvable, it was seen in several experimental tests and is evidently characteristic of the low and high coverage oxygen adsorption states on Pt(100). Since the high coverage state seems chemically different, it is of particular interest to determine whether any of the oxygen penetrates to the subsurface region of the platinum. We addressed this question by varying the takeoff angle, the angle of electron emission from the sample into the analyzer. Variation of the emission angle affects the surface sensitivity by changing the effective escape depth of the photoelectrons. Although the actual physical situation is complicated (17), the formal expression for the distance d below the surface where an electron originates is from

simple geometrical considerations given by,

$$d = \ell \cos \Theta \qquad [2]$$

where ℓ is the distance traversed by the electron before escape into the vacuum and Θ is given by Fig. 1. Figure 6 presents data for the O1s and Pt4p lines taken at three different values of Θ. All three spectra were collected consecutively after exposing the surface under the usual conditions to produce the high coverage state. The data were normalized so that the Pt4p peaks are the same height, and a spectrum at $\Theta = 84°$ was repeated after spectrum c to check for adlayer degradation, which was $< 7\%$. There is obviously a dramatic enhancement of emission from the O1s level for glancing electron take-off compared to $\Theta = 45°$, indicating the expected enhancement of surface sensitivity of the Pt4p photoemission at glancing take-off. Figure 7 compares the data of Fig. 6 to spectra for carbon monoxide adsorption, where it is certain that all the O1s emission originates from oxygen atoms <u>on</u> the surface, and to oxygen observed with new crystals before the argon sputtering cycles (see Section II). This latter oxygen state survives heating to $\gtrsim$ 1000 K and is probably due to Si or Ca contamination; these contaminant oxides are generally thought to reside in the subsurface region (22). It is clear that the adsorbed oxygen and CO vary similarly (almost identically) with Θ, while the contaminant oxide signal shows a quite different pattern. Thus, we conclude that the high coverage state formed at 570 K does not exhibit significant bulk penetration by oxygen. Some penetration of the surface such as by a place-exchange type restructuring of some of the Pt atoms in the first two atomic layers cannot be ruled out, however.

The variable take-off spectra could also be used to estimate, independently, the oxygen coverage. By using ratios of the areas under the O1s and Pt4p peaks, the effects of x-ray flux, spectrometer response function, etc. are made to cancel. The peak areas then need only to be corrected for the relative photoelectron cross-sections (23) and the effective escape depth for the Pt4p photoelectrons, so that

$$N_o \approx \left(\frac{I(O1s)/\sigma(O1s)}{I(Pt4p)/\sigma(Pt4p)}\right) (\ell \cos\Theta) N_{Pt} \qquad [3]$$

where N_{Pt} and N_o are the number densities per unit area of platinum and oxygen, and ℓ is the characteristic mean-free path. Using the three intensity ratios for the three different take-off angles and assuming 16 Å for the inelastic mean free path for the Pt4p photoelectrons (24), the oxygen coverage from equation [3] was found to be 1.1 (±0.3) x 10^{15} atoms/cm^2 for the high coverage state, which is consistent with the coverage obtained from the TDS peak areas.

We also examine the effects of oxygen adsorption on the Pt4f lines. The data in Fig. 8 are for the clean platinum surface, a surface exposed to oxygen under conditions (~10^{-3} Pa at 570 K for 300 sec.) that produce the high coverage state, and the difference spectrum for these two. Curves a and b are plotted on identical vertical scales. The spectral lines generated from the oxygen covered surface are shifted by $\Delta E \approx 0.3$ eV to higher binding energy and are attenuated compared to the clean surface data. Looking at the difference spectrum, in addition to attenuation (negative differences at 70.5 and 74 eV) new features appear as positive differences at 72 and 75 eV, corresponding to a shift of about 1 eV to higher binding energy of some fraction of the Pt atoms in the surface

region. The data in Fig. 8 were collected at $\Theta = 84°$ to maximize surface sensitivity. Spectra were also taken at $\Theta = 74°$, $\Theta = 65°$, and $\Theta = 45°$, and the features at 72 and 75 eV became progressively less pronounced with increasing take-off angle, e.g. at $\Theta = 45°$ there was essentially no difference between the Pt4f spectra for clean and oxygen covered surfaces. The + 1 eV binding energy shift therefore appears to be associated with the first-layer Pt atoms.

2. Pt(111) Surface

XPS data were also collected for oxygen adsorption on the Pt(111) surface as a function of coverage and take-off angle. For the O1s spectra equivalent to Fig. 5, which compared the high and low coverage states on Pt(100), the only difference between the two spectra was the area under the curves, i.e. the binding energy was the same in both cases, 530.8 eV. The Pt4f spectra for Pt(111) after oxygen dosing to produce the high coverage state were very similar to the Pt(100) spectra shown in Fig. 8.

IV. Discussion

We start by considering the kinetics of adsorption into the low coverage state on Pt(100). Two different analyses yield a desorption energy $E \approx 115$ kJ/mole; only one (20) assumes that E and k_0 are coverage independent, but both assume kinetics governed by the form of equation [1]. The isotherm analysis indicates that m = 2, but this cannot be implicitly relied on due to scatter in the data. Using the desorption energy and coverage estimate to calculate the pre-exponential, k_0, we obtain $k_0 \sim 10^{-8}$ cm^2/sec. While this is in general agreement with a previous estimate (4) for O_2/Pt(111), it is anomalously low compared to the usually expected value (25) by several orders of magnitude. It is now well

known (26) that transient precursor states, lateral adatom interactions, etc., can cause radical deviations from the Arrhenius form, eq. [1]. If this is the case, then it could account for the low k_o value (which would mean that desorption energy is significantly in error). There is no independent evidence on which to base that assumption, so we tantatively quote our value of E with the caveat that future work may show conclusively that it was calculated from erroneous premises. As mentioned in Section III, the initial low temperature sticking coefficient for oxygen on UHV annealed Pt(100) we report is an order of magnitude higher than Kneringer and Netzer (15) and several earlier workers reported virtually no adsorption of oxygen on UHV annealed Pt(100). The most probably explanation for these discrepancies is the influence of clean-off reactions, especially due to CO as described by Barteau, et al. (16). The kinetics of adsorption into the high coverage state cannot be characterized at this time. It is obvious that this is not a simple first or second order reaction, but we need more information to model the mechanism causing the asymmetric lineshape. Barteau, et al. (16) were able to fit their data using a coverage dependent desorption energy, but this was an ad hoc assumption not based on a physical model.

It is very interesting to compare the O_2/Pt(100) thermal desorption spectra of Kneringer and Netzer (15), Barteau, et al. (16), and the present study. Kneringer and Netzer exposed the sample at ambient temperature to ~ 10^{-3} Pa oxygen. They observed a major thermal desorption peak centered

at 790 K and two smaller features at higher temperature (960 K and 1070 K) and identified all three as second order reactions with a total coverage of 0.25 monolayers. Barteau, et al. dosed their sample with ~10^{-4} Pa oxygen at T_s = 585 K and observed quite different behavior: a very sharp peak at 676 K (which they call "autocatalytic") and another feature at 709 K (denoted as first order), the total coverage quoted as 0.66 monolayers. The present work clearly shows that these different TDS observations arise from the difference in dosing conditions employed.

The high coverage state on Pt(111) had not been produced in prior work by the use of our dosing conditions, but several investigators have produced similar high oxygen coverages by other means, e.g. gas-phase atomization of oxygen or dosing with NO_2 (27). In these works, they also observed an asymmetric peak shape like that in Fig. 4, and by virtue of vibration spectroscopy and isotopic mixing studies concluded that the high coverage state was not chemically different from the low coverage state. This conclusion is in agreement with our own based on the XPS data reported here.

For oxygen adsorbed on Pt(100), the O1s binding energy shows a small shift to <u>lower</u> binding energy in going from low to high coverage; oxygen on Pt(111) did not show this shift. Previous XPS studies have shown that Fermi level referenced binding energies (E_b^F) for oxygen on metals are not unambiguously correlated to the chemical state of the oxygen. As examples, we cite the study of oxygen on aluminum (29) where the transition from the chemisorbed state to the anionic ("oxide") state caused a shift in E_b^F for O1s to higher binding energy, while for oxygen on nickel (30) the shift was to lower binding energy, and for oxygen on tungsten (31) there was essentially no shift. Krishnan, et al. (30) have argued

that binding energies for O1s that are more consistent with chemical intuition are obtained if one uses binding energies referenced to the vacuum level; i.e. $E_b^V = E_b^F + \Phi$. We have studied the changes in work function produced by oxygen chemisorption (28) and found that the work function increased monotonically with coverage with a maximum value for $\Delta\Phi$ of ~ 0.3 eV on Pt(111) and ~ 0.9 eV on Pt(100) at near monolayer coverages. Using these work function measurements, the vacuum referenced binding energies actually shift to slightly higher binding energy with increasing coverage. In terms of absolute values at high oxygen coverages, E_b^V ~ 536.7 eV for (111) and ~ 536.6 eV for (100). In comparison to the vacuum referenced binding energies for oxygen on nickel reported by Krishnan, et al., the high coverage O1s binding energies for oxygen on Pt are ~ 2 eV higher than for the "oxidized" nickel surface. While these binding energy differences reflect the combined effects of chemical bonding and extra-atomic relaxation, these differences do indicate it is unlikely that the high coverage state of oxygen on Pt is oxidic. The formation of oxidic (anionic) oxygen necessitates charge transfer from Pt nearest neighbors, and the formation of at least partially cationic Pt surface atoms. The appearance of the Pt4f difference spectrum for Pt(100) suggests a possible cationic shift (+ 1 eV) for some fraction of the total Pt surface. Very similar difference curves were obtained by Norton, et al. (3) for a Pt(100) surface after extremely large doses (10^7 L O_2) at T_s = 550 K. Norton, et al. interpreted their result as the formation of platinum oxide at the surface. We feel that this is not the correct interpretation of the difference curves and the chemical shifts derived from them. The variable takee-off angle data indicate that the oxygen

resides on the surface, and the Pt4f chemical shifts are smaller than values reported in the literature (32) for PtO and PtO_2. There is adequate precedent in the literature to indicate that the chemisorption of electron withdrawing adsorbates like oxygen and carbon monoxide induce ca. + 1 eV shifts to Pt4f levels of surface atoms. Recent work by Apai, et al. (33) and Shek, et al. (34) on CO/Pt report Pt4f levels for surface atoms are shifted by - 0.4 eV relative to the 4f levels of bulk atoms and that CO chemisorption induces ~ 1.2 eV shift to higher binding energy in these levels. Analogously, the decreases and increases in intensity shown by the oxygen difference spectrum in Fig. 9 can also be interpreted as the shift of a feature from an energy lower than the main peak (difference minimum is at 70.5) to an energy higher than the main peak (difference maximum is at 72 eV), i.e. a surface atom core level shift of ca. 1.5 eV. We feel the most reasonable interpretation of the Pt4f data for the high coverage state of oxygen is in terms of chemisorption induced surface core level shift characteristic of an electron withdrawing adsorbate.

Acknowledgment

This work was supported by the Assistant Secretary for Fossil Energy, Office of Fuel Cells, Advanced Concepts Division of the U.S. Department of Energy under Contract No. DE-AC03-76SF00098 through the Fuel Cell Project Office, NASA Lewis Research Center, Cleveland, Ohio.

References

1. P. R. Norton, Surf. Sci. 47 98 (1975).

2. P. R. Norton, J. Catalysis 36 211 (1975).

3. P. R. Norton, R. L. Tapping, and J. W. Goodale, J. Vac. Sci. Technol. 14 446 (1977).

4. J. L. Gland, Surf. Sci. 93 487 (1980).

5. J. L. Gland, B. A. Sexton, and G. B. Fisher, Surf. Sci. 95 587 (1980).

6. D. R. Monroe and R. P. Merrill, J. Catalysis 65 461 (1980).

7. C. T. Campbell, G. Ertl, H. Kuipers, and J. Segner, Surf. Sci. 107 220 (1981).

8. D. M. Collins and W. E. Spicer, Surf. Sci. 69 85 (1977).

9. D. M. Collins and W. E. Spicer, Surf. Sci. 69 114 (1977).

10. J. Küppers and G. Ertl, Surf. Sci. 77 L647 (1978).

11. J. N. Miller, D. T. Ling, I. Lindau, D. M. Collins and W. E. Spicer, Surf. Sci. 77 L651 (1978).

12. C. R. Helms, H. P. Bonzel and S. Kelemen, J. Chem. Phys. 65 1773 (1976).

13. G. Pirug, G. Broden, and H. P. Bonzel, Proc. Third International Conf. on Solid Surfaces, Vienna, 1977, p. 907.

14. A. C. Balazs and K. H. Johnson, Surf. Sci. 114 197 (1982).

15. G. Kneringer and F. P. Netzer, Surf. Sci. 49 125 (1975).

16. M. A. Barteau, E. I. Ko, and R. J. Madix, Surf. Sci. 102 99 (1981).

17. C. S. Fadley, J. Elect. Spectr. 5 725 (1974).

18. C. D. Wagner, in Applied Surface Analysis, ed. by T. L. Barr and L. E. Davis (ASTM Technical Publication 699, Baltimore 1980) p. 137.

19. P. R. Norton, J. A. Davies, and T. E. Jackman, Surface Science 122, L593 (1982).

20. P. A. Redhead, Vacuum 12, 203 (1962).

21. D. A. King, Surf. Sci. 47, 384 (1975).

22. H. Niehus and G. Comsa, Surf. Sci. 102, L14 (1981).

23. J. H. Scofield, J. Elect. Spect. 8, 129 (1976).

24. C. J. Powell, Surf. Sci. 44, 29 (1974).

25. For a discussion on prefactor values, see the review by D. Menzel in Interactions on Metal Surfaces, ed. by R. Gomer (Springer-Verlag, New York, Heidelberg, Berlin 1975). p. 101.

26. See, e.g., the review by D. A. King, in Chemistry and Physics of Solid Surfaces, Vol. 2, ed. by R. Vanselow (CRC Press, Boca Raton, Florida (1979). p. 87.

27. H. Steininger, S. Lehwald, and H. Ibach, Surf. Sci. 123, 1 (1982)' D. Dahlgren and J. C. Hemminger, Surf. Sci. 123, L739 (1983).

28. G. N. Derry and P. N. Ross, Lawrence Berkeley Laboratory Report LBL-16409.

29. A. M. Bradshaw, P. Hoffman and W. Wyrobisch, Surf. Sci. 68, 269 (1977).

30. N. G. Krishnan, W. N. Delgas and W. D. Robertson, Surf. Sci. 57, 1 (1976).

31. J. T. Yates, T. E. Madey and N. E. Erickson, Surf. Sci. 43, 257 (1974).

32. M. Alnot and A. Cassuto, Surf. Sci. 112, 325 (1981).

33. G. Apai, R. C. Baetzold, E. Shustorovich and R. Jaeger, Surf. Sci. 116, L191 (1982).

34. M. L. Shek, P. M. Stefan, C. Binns, I. Lindau and W. E. Spicer, Surf. Sci. 115, L81 (1982).

Figure Captions

Fig. 1. Experimental geometry, defining the polar angle Θ for electron take-off by the electron energy analyzer.

Fig. 2. Analysis of the low coverage thermal desorption data for Pt(100), showing coverage dependence with exposure (a) and peak temperature variation with coverage (b); the line in b is a least squares fit to the data points.

Fig. 3. Oxygen thermal desorption from Pt(100) for the high (curve a) and low (curve b) coverage states (see text for exposure conditions).

Fig. 4. Oxygen thermal desorption from Pt(111) for the high (curve a) and low (curve b) coverage states (see text for exposure conditions).

Fig. 5. XPS data on the O1s level for oxygen on Pt(100) in the high coverage (curve a) and low coverage (curve b) states; data taken at $\Theta = 84°$.

Fig. 6. XPS data for the high coverage state on Pt(100) collected at varying electron emission angles; curve a is for $\Theta = 84°$, curve b is for $\Theta = 70°$, curve c is for $\Theta = 45°$.

Fig. 7. Comparison of the areas under the O1s and Pt4p curves at $\Theta = 84°$, 70°, and 45° for the high coverage oxygen state, CO adsorption, and a subsurface contaminant oxide.

Fig. 8. XPS data on the Pt4f lines at $\Theta = 84°$ for the clean surface (curve a), the high coverage state (curve b), and the difference spectrum (curve c).

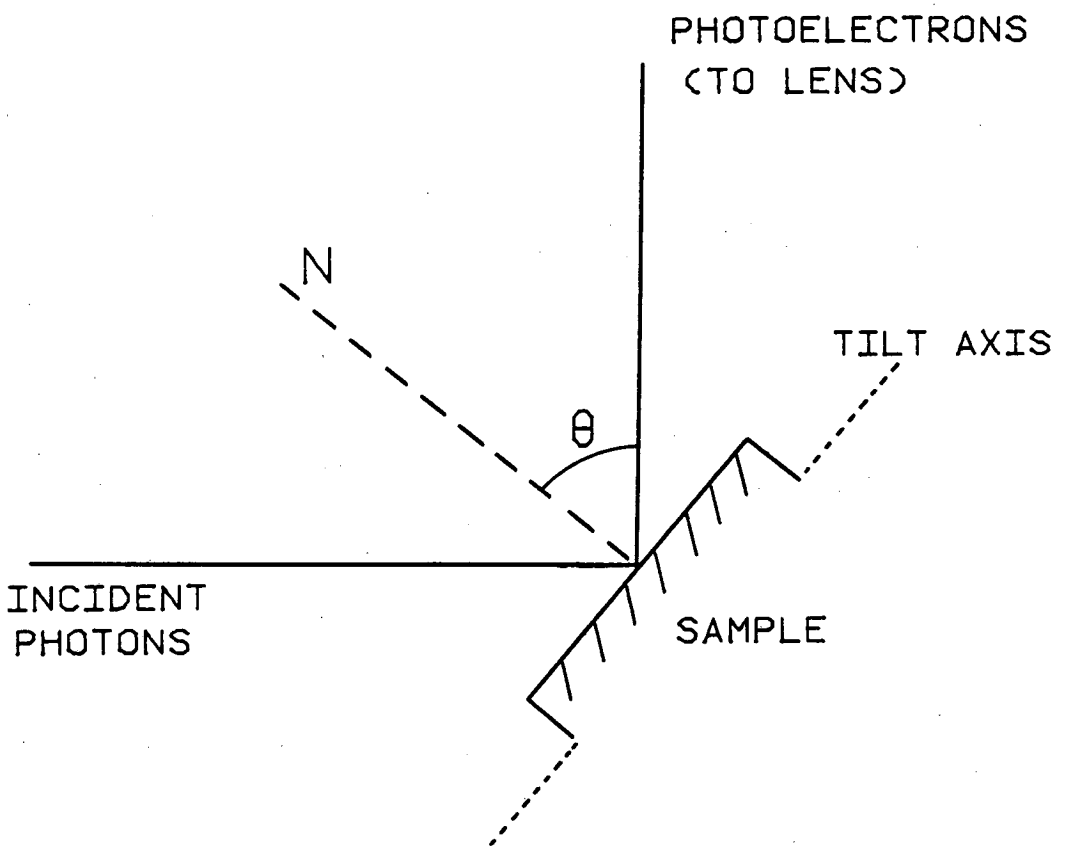

SAMPLE GEOMETRY

XBL 828-11204

Fig. 1

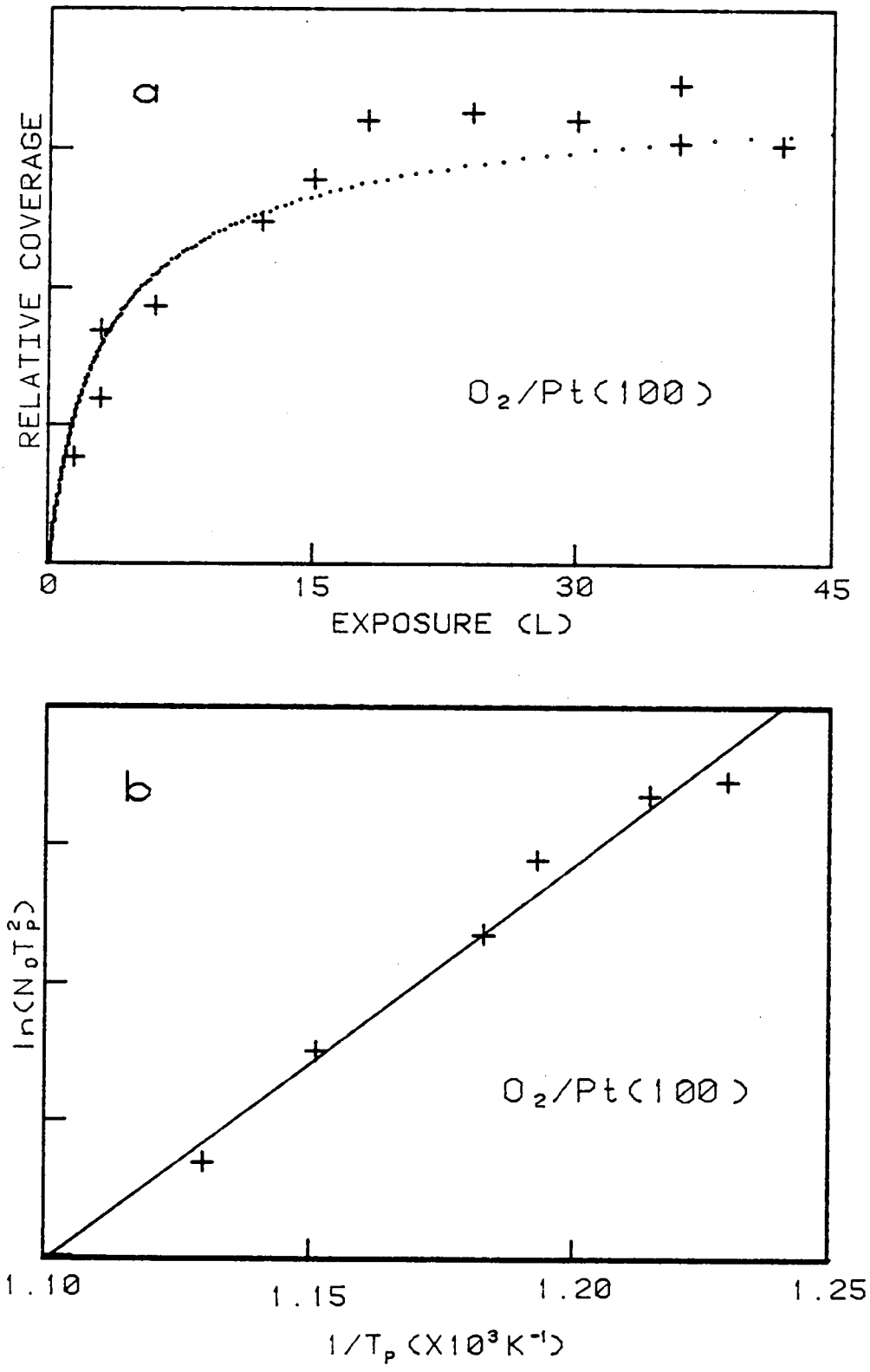

XBL 828-11206

Fig. 2

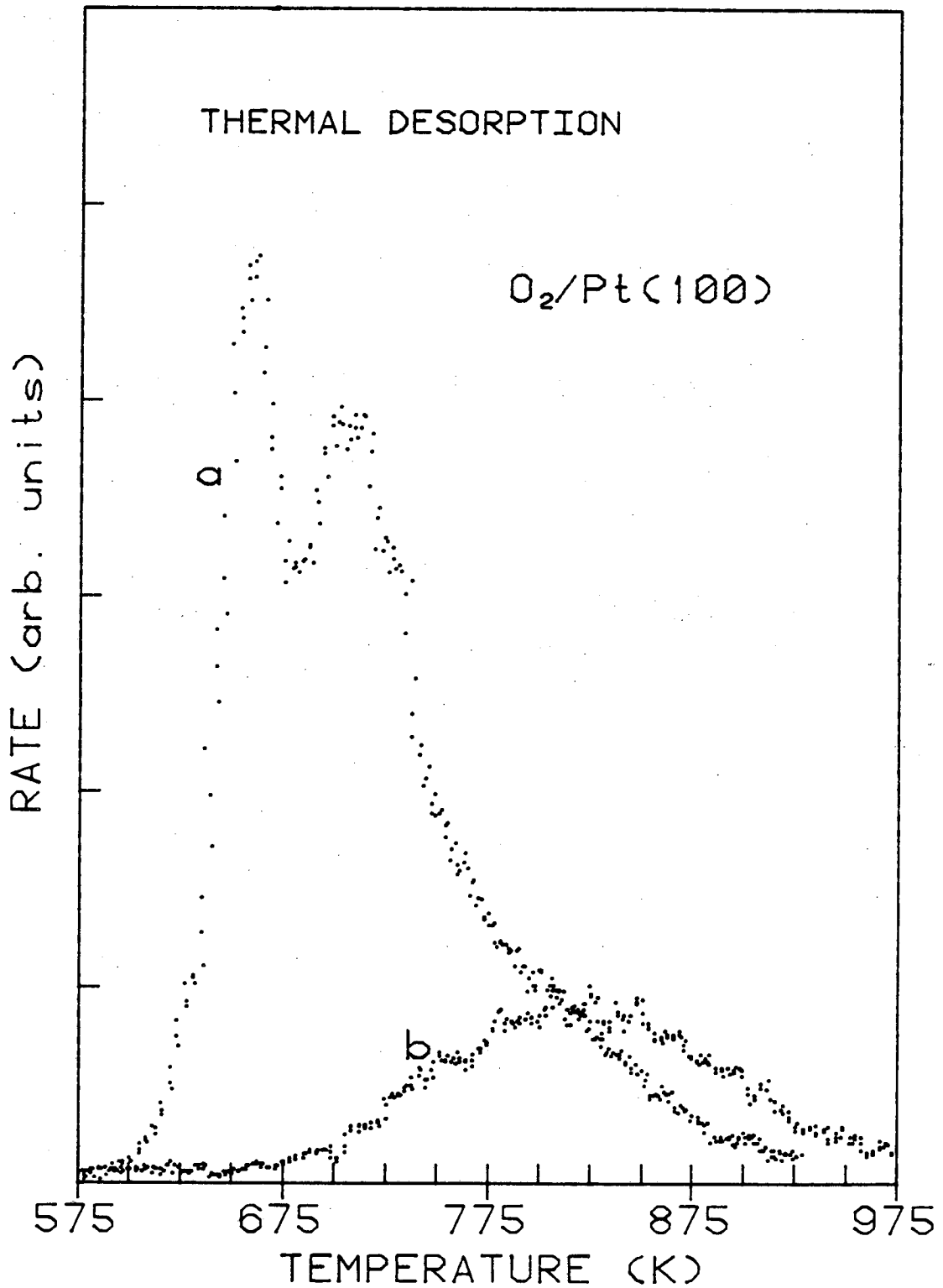

XBL 828-11209

Fig. 3

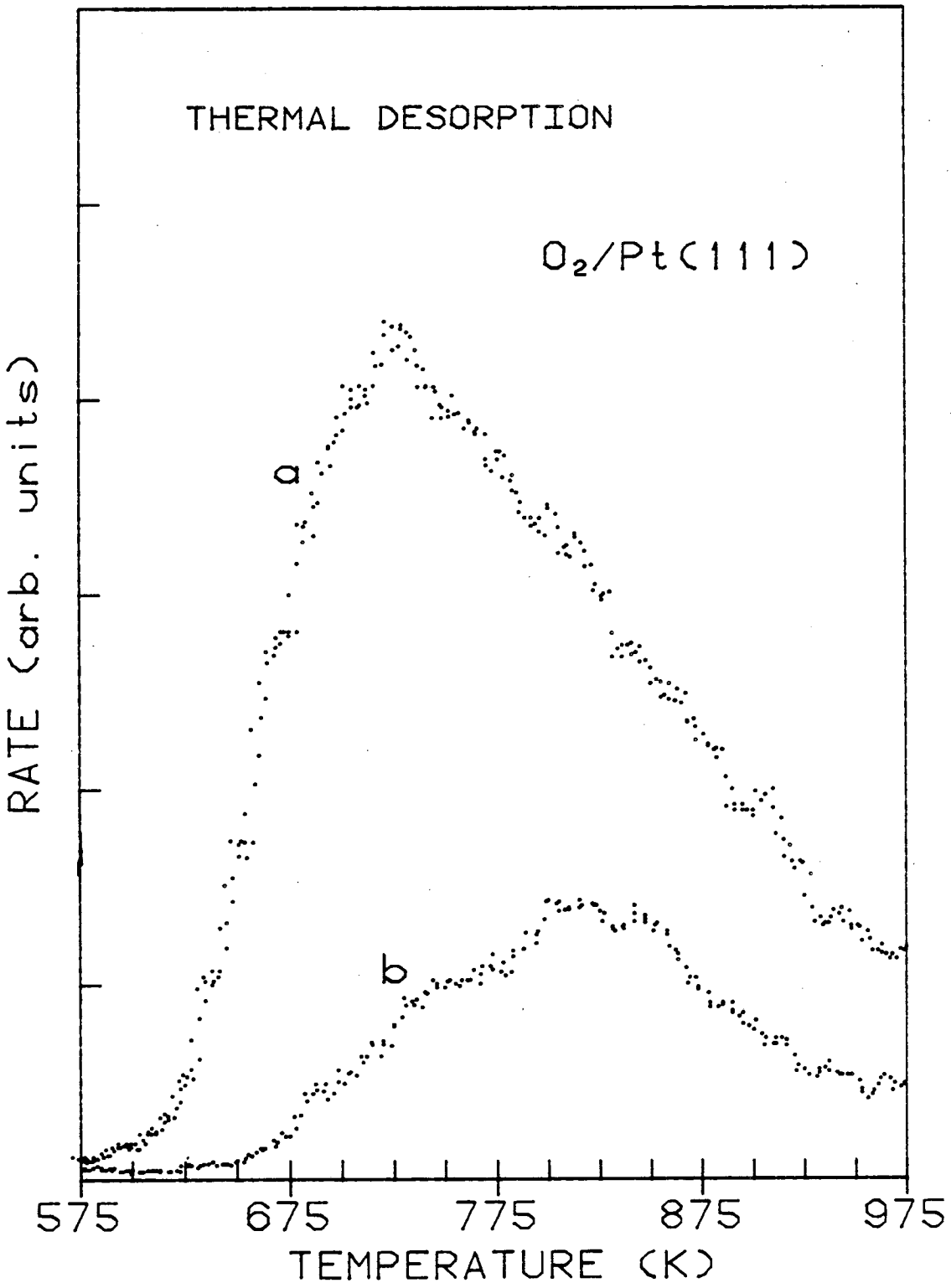

XBL 828-11208

Fig. 4

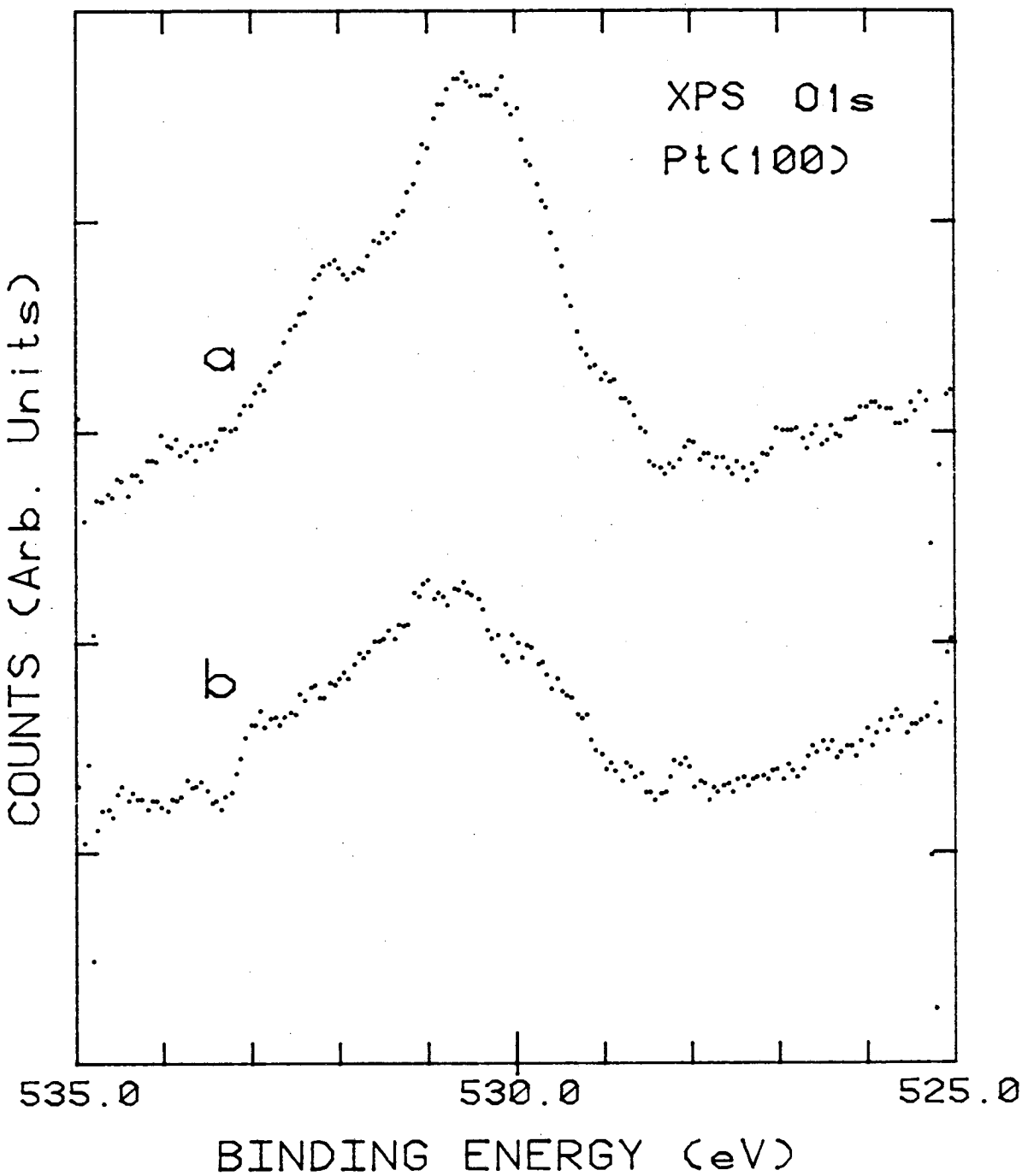

XBL 828-11214

Fig. 5

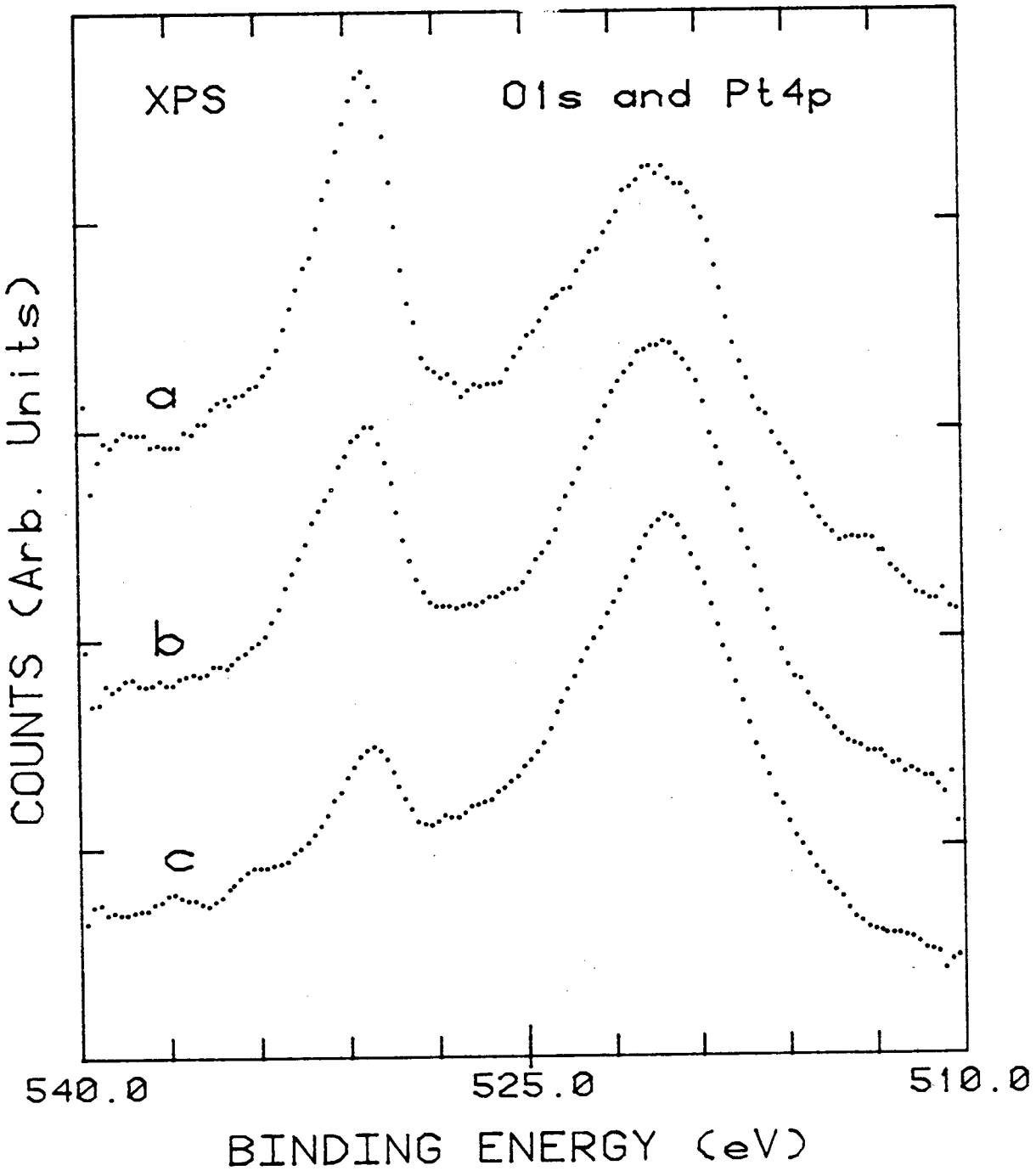

XBL 828-11215

Fig. 6

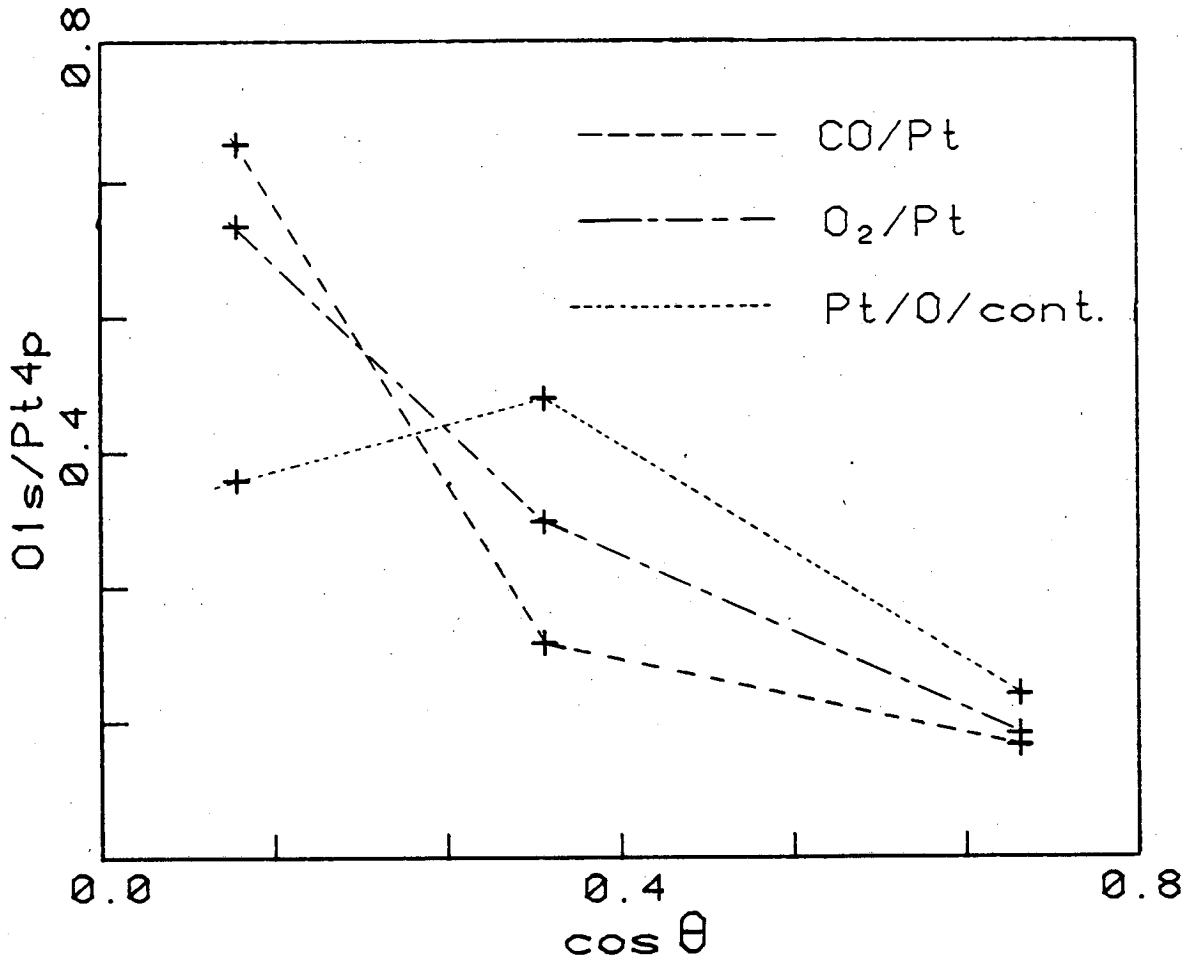

XBL 828-11205

Fig. 7

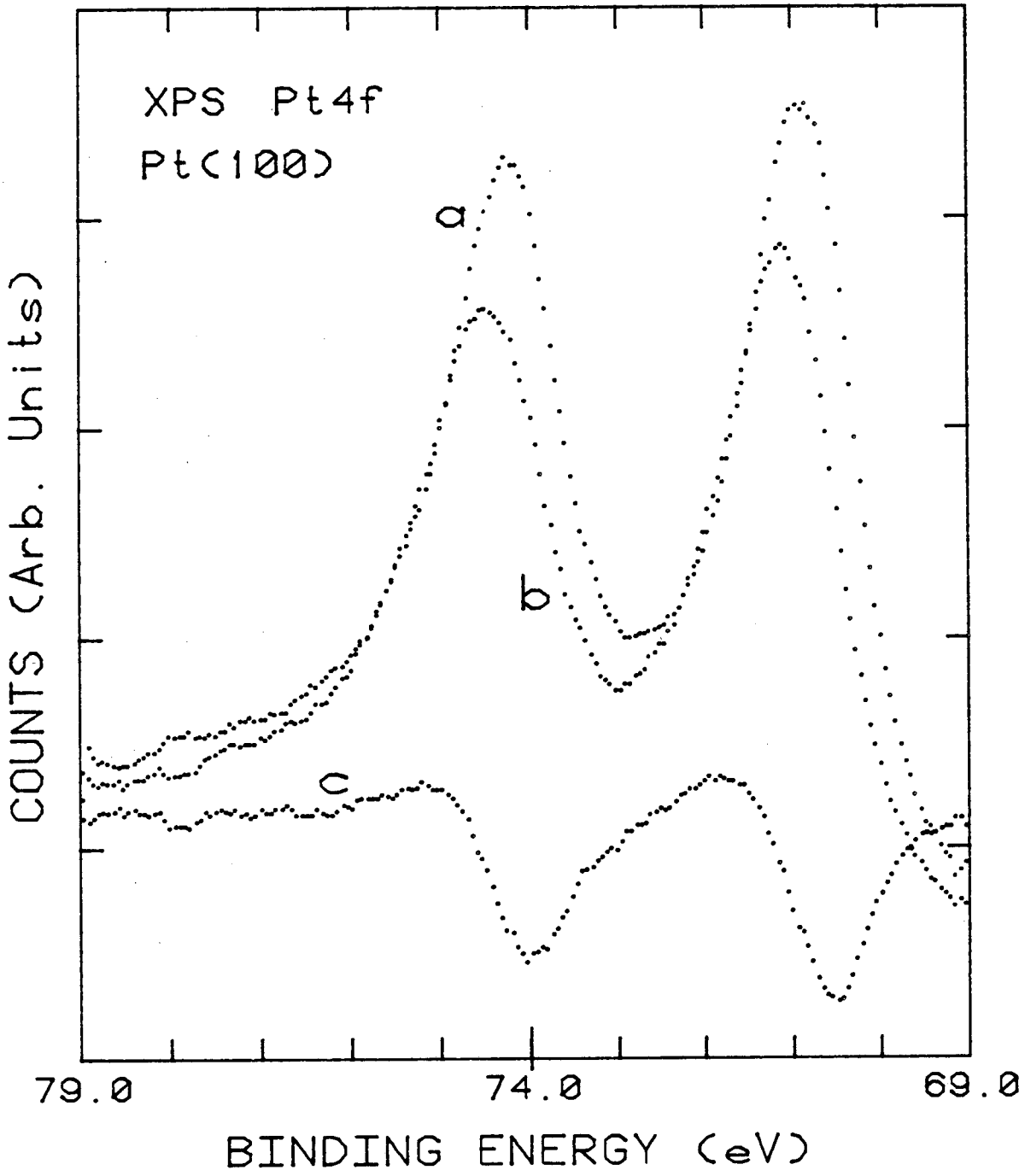

XBL 828-11212

Fig. 8

This report was done with support from the Department of Energy. Any conclusions or opinions expressed in this report represent solely those of the author(s) and not necessarily those of The Regents of the University of California, the Lawrence Berkeley Laboratory or the Department of Energy.

Reference to a company or product name does not imply approval or recommendation of the product by the University of California or the U.S. Department of Energy to the exclusion of others that may be suitable.

TECHNICAL INFORMATION DEPARTMENT
LAWRENCE BERKELEY LABORATORY
UNIVERSITY OF CALIFORNIA
BERKELEY, CALIFORNIA 94720